



Research Article

Adaptive control of 5 DOF upper-limb exoskeleton robot with improved safety[☆]Hao-Bo Kang^{a,*}, Jian-Hui Wang^b^a Northeastern University, Shenyang, China^b College of Information Science and Engineering, Northeastern University, China

ARTICLE INFO

Article history:

Received 2 January 2013

Received in revised form

25 April 2013

Accepted 9 May 2013

Available online 30 July 2013

This paper was recommended for publication by Dr. Jeff Pieper

Keywords:

Adaptive control

Safety requirement

Observer-based control

Robotics

ABSTRACT

This paper studies an adaptive control strategy for a class of 5 DOF upper-limb exoskeleton robot with a special safety consideration. The safety requirement plays a critical role in the clinical treatment when assisting patients with shoulder, elbow and wrist joint movements. With the objective of assuring the tracking performance of the pre-specified operations, the proposed adaptive controller is firstly designed to be robust to the model uncertainties. To further improve the safety and fault-tolerance in the presence of unknown large parameter variances or even actuator faults, the adaptive controller is on-line updated according to the information provided by an adaptive observer without additional sensors. An output tracking performance is well achieved with a tunable error bound. The experimental example also verifies the effectiveness of the proposed control scheme.

© 2013 ISA. Published by Elsevier Ltd. All rights reserved.

1. Introduction

Recent research reports in clinical treatment for upper-limb rehabilitation proved that robot-aided therapy is a credible approach to recover motor control of the proximal upper limb and amend functional outcomes [1,2]. Compared with the conventional therapies, electromechanical and robotic devices are able to give an increased motivation to train and the opportunity for independent exercise [1]. In fact, robot-aided therapy is more practical in the frequency of movement repetitions. Thus many robotic devices were applied to provide passive arm movements, including the actions of moving the subject's limb through a pre-determined trajectory (i.e., trajectory tracking) [3–8].

Various control objectives were achieved by implementing modern control techniques such as optimal control method [4], robust control approach [5], and the conventional PID control method [6]. Among these control objectives, a consistent high dynamic tracking performance is pursued to maneuver the exoskeleton as a basic requirement. Because human arm movement is nonlinear in nature, conventional linear control approaches have their limitations while dealing with an upper-limb exoskeleton

robot. Therefore, the idea of nonlinear control for upper-limb exoskeleton robot has motivated a series of works of nonlinear control strategies, e.g., computed torque control [7], sliding mode control method [8], and iterative learning control scheme [9], gain scheduling control approach [10], to name a few. But most of the existing results of nonlinear control for upper-limb rehabilitation robot are developed for the simplified dynamic models, e.g., typical simplified models ignoring the mass/inertia or the centrifugal terms [7–10]. To guarantee its reliability in the practical situation, the design of robotic controller must take into consideration the modeling errors and the unknown uncertainties. Unfortunately, the conventional controllers is not ideal because they lack the self-adjustment ability to cope with parameter variances, e.g., the mass of the human upper-limb varying from person to person.

On the other hand, to cope with nonlinearities and uncertainties, the nonlinear adaptive control strategies [11,17–21] have gained a great achievement in various nonlinear systems such as robotic systems [12–14]. Since its application in exoskeleton robots is relatively new, the adaptive robust control technique has a good potential to deliver a solution to guarantee consistently high dynamic tracking performance in the presence of uncertainties. For the participation of patients, the safety requirement cannot be neglected during rehabilitation training, especially in the unintended situation. To achieve safety requirement, the hardware equipments such as travel limiting contact or lead limit switch are commonly installed in the rehabilitation robot. But these

[☆]The work is supported by National Natural Science Fund China under grant 61104015, Liaoning Science and Technology Program under Grant 2010020176-301 and Shenyang Municipal Fund under Grant F10-2D5-1-57.

* Corresponding author. Tel.: +86 13555849510.

E-mail addresses: kangta_apple@163.com, mathworm@126.com (H.-B. Kang).

arrangements cannot completely guarantee the safety of the patients in the presence of large parameter variance and the hardware malfunctions, even actuator faults. Implementing the adaptive controller should consider the reliability and fault-tolerance in such situations when getting high accuracy.

The above considerations give a strong motivation of developing an adaptive controller design method to achieve high tracking performance and safety requirement in the presence of nonlinearities and uncertainties. The available information is the position, the estimation of velocity and acceleration provided by an adaptive observer. To deal with the unknown uncertainties satisfying the linear growth condition, the observer is adjusted by a dynamic gain. The proposed updated law of observer gain is dependant on a logic-switching parameter of the position measurement. To improve the safety of the whole robotic system, the effect of the hardware malfunctions, even actuator faults is described in a unified model and thus automatically accommodated. The proposed control scheme is called ‘adaptive’ in the sense that once the controller is developed, it can regulate all systems that have nonlinearities satisfying the imposed linear growth condition with different bounds. Thus, the control parameters are not needed to be redesigned each time.

In the next section of this paper, the dynamics of the considered 5 DOF upper-limb exoskeleton robot is described with control objective. The state space model of 5 DOF upper-limb exoskeleton robot is described and an adaptive control strategy is presented in Section 3. In Section 4, an experimental result is presented, and finally the paper ends with a conclusion in Section 5.

2. Architecture of the considered 5 DOF upper-limb exoskeleton robot

2.1. Robot dynamics

In this paper, the research object of 5 DOF exoskeleton upper-limb rehabilitation robot is shown in Fig. 1. Based on anatomy of human upper-limb, the rehabilitation robot simulates the most important 5 DOF in the human upper-limb movements: shoulder abduction/adduction, shoulder flexion/extension, the elbow flexion/extension, wrist flexion/extension and internal rotation/external rotation. The robot realizes single-joint movements and complex motions of multi-joint in training of the daily living for

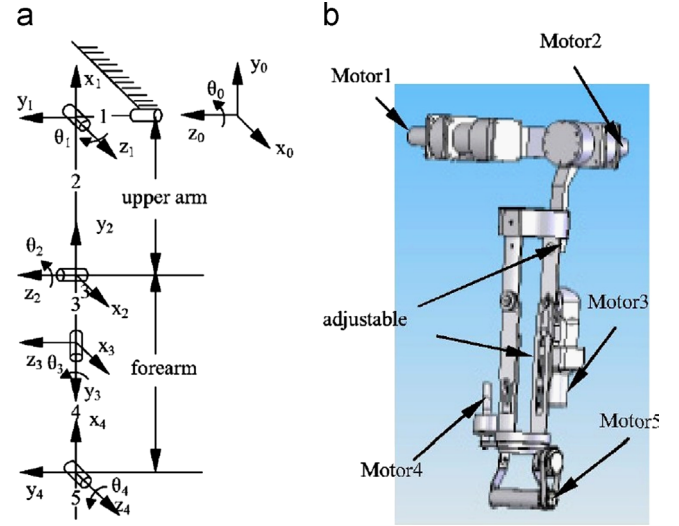


Fig. 2. Schematic diagram of a 5 DOF upper-limb exoskeleton robot.

patients, such as pointing nose, pull trousers and so on. At each axis, different servomotor drivers are chosen to satisfy various driving power. Reasonable place of five motors saves the space of robot (shown in Fig. 1). Three Panasonic AC servo motor drivers are installed in shoulder and elbow joints because of their great moment power to actuating the robot and human upper limb. Two joints of wrist are driven by two maxon DC servo motor with smaller moment. Optical encoder signals read from series of PC record the absolute positions of the device and the angles of the joints. MAC-3002SSP4 motor control card is used to control motor motion. All control algorithms have been developed on a PC using VC6.0 (Fig. 2).

The dynamic behavior of the 5 DOF upper-limb exoskeleton robot can be described by the rigid body dynamic equation [15] as follows:

$$M(q)\ddot{q} + C(q, \dot{q})\dot{q} + G(q) + \tau_d = \tau, \quad (1)$$

where $q, \dot{q}, \ddot{q} \in R^5$ represent the position, velocity, $\tau \in R^5$ is the joint torques and $\tau_d \in R^5$ is the disturbance torques. The generalized inertia matrix $M(q) \in R^{5 \times 5}$ is computed as

$$M(q) = \begin{bmatrix} M_{11} & M_{12} & M_{13} & 0 & 0 \\ M_{21} & M_{22} & M_{23} & 0 & 0 \\ M_{31} & M_{32} & M_{33} & 0 & M_{35} \\ 0 & 0 & 0 & M_{44} & 0 \\ 0 & 0 & M_{53} & 0 & M_{55} \end{bmatrix}$$

with

$$\begin{aligned} M_{11} = & I_2 + I_{19} + I_3 \cos^2(q_2) + I_4 \sin^2(q_2 + q_3) \\ & + I_5 \sin(q_2 + q_3) \cos(q_2 + q_3) + I_6 \sin(q_2) \cos(q_2) \\ & + I_7 \sin^2(q_2 + q_3) + 2 + I_8 \cos(q_2) \sin(q_2 + q_3) \\ & + I_9 \cos(q_2) \cos(q_2 + q_3) + I_{10} \sin^2(q_2 + q_3) \\ & + I_{11} \cos(q_2) \sin(q_2 + q_3) + I_{12} \sin(q_2 + q_3) \cos(q_2 + q_3), \\ M_{12} = & M_{21} = I_{13} \sin(q_2) + I_{14} \cos(q_2 + q_3) + I_{15} \cos(q_2) \\ & + I_{16} \sin(q_2 + q_3) - I_{17} \cos(q_2 + q_3), \\ M_{13} = & M_{31} = I_{14} \cos(q_2 + q_3) + I_{16} \sin(q_2 + q_3) - I_{17} \cos(q_2 + q_3), \\ M_{22} = & I_{18} + I_{19} + I_{20} + 2I_8 \sin(q_3) + I_9 \cos(q_2) + I_{10} + I_{11} \sin(q_3), \\ M_{23} = & M_{32} = I_8 \sin(q_3) + I_{20} + I_9 \cos(q_3) + I_{11} \sin(q_3) + 2I_{10}, \\ M_{33} = & I_{m3} + I_{20} + 2I_{10}, M_{35} = M_{53} = I_{10} + I_{21}, \\ M_{44} = & I_{22} + I_{23}, M_{55} = I_{24} + I_{21}, \end{aligned}$$



Fig. 1. Photograph of a real 5 DOF upper-limb exoskeleton robot.

and the carioles/centripetal matrix $C(q, \dot{q}) \in \mathbb{R}^{5 \times 5}$ is calculated as

$$C(q, \dot{q}) = \begin{bmatrix} c_1 \dot{q}_2 & c_2 \dot{q}_3 + c_3 \dot{q}_2 & c_4 \dot{q}_2 + c_5 \dot{q}_3 & 0 & 0 \\ c_6 \dot{q}_1 & c_7 \dot{q}_3 & c_8 \dot{q}_3 & 0 & 0 \\ c_9 \dot{q}_1 & c_9 \dot{q}_2 & 0 & 0 & 0 \\ c_{10} \dot{q}_2 & 0 & c_{11} \dot{q}_1 & 0 & 0 \\ 0 & c_{12} \dot{q}_2 & 0 & 0 & 0 \end{bmatrix}$$

where

$$\begin{aligned} c_1 &= 2[-I_3 \sin(q_2) \cos(q_2) + I_8 \cos(2q_2 + q_3) \\ &\quad + I_4 \sin(q_2 + q_3) \cos(q_2) - I_9 \sin(2q_2 + q_3) - I_{10} 2 \sin(q_2 + q_3) \\ &\quad + I_{11} \cos(2q_2 + q_3) + I_7 \sin(q_2 + q_3) \cos(q_2 + q_3) \\ &\quad + I_{12}(1 - 2 \sin(q_2 + q_3) \sin(q_2 + q_3))] \\ &\quad + I_5(1 - 2 \sin(q_2 + q_3) + I_6(1 - 2 \sin^2(q_2))), \end{aligned}$$

$$c_2 = 2[-I_{14} \sin(q_2 + q_3) + I_{16} \cos(q_2 + q_3) + I_{17} \sin(q_2 + q_3)],$$

$$\begin{aligned} c_3 &= I_{13} \cos(q_2) - I_{14} \sin(q_2 + q_3) - I_{15} \sin(q_2) \\ &\quad + I_{16} \cos(q_2 + q_3) + I_{17} \sin(q_2 + q_3), \end{aligned}$$

$$\begin{aligned} c_4 &= 2[I_8 \cos(q_2) \cos(q_2 + q_3) + I_4 \sin(q_2 + q_3) \cos(q_2 + q_3) \\ &\quad - I_9 \cos(q_2) \sin(2q_2) + I_{10} 2 \sin(q_2 + q_3) \cos(q_2 + q_3) \\ &\quad + I_{11} \cos(q_2) \cos(q_2 + q_3) + I_7 \sin(q_2 + q_3) \cos(q_2 + q_3) \\ &\quad + I_{12}(1 - 2 \sin(q_2 + q_3) \sin(q_2 + q_3))] \\ &\quad + I_5(1 - 2 \sin(q_2 + q_3) \sin(q_2 + q_3)) \end{aligned}$$

$$c_5 = 0.5c_2,$$

$$c_6 = -0.5c_1,$$

$$c_7 = 2[-2I_9 \sin(q_3) + I_8 \cos(q_3) + I_{11} \cos(q_3)],$$

$$c_8 = -0.5c_4,$$

$$\begin{aligned} c_9 &= \sin(q_2 + q_3) \cos(q_2 + q_3) - 2I_{10} \sin(q_2 + q_3) \cos(q_2 + q_3) \\ &\quad - I_{11} \cos(q_2) \cos(q_2 + q_3) - I_{12} \cos^2(q_2 + q_3), \end{aligned}$$

$$c_{10} = -[I_{23} \sin(q_2 + q_3) + I_{19} \sin(q_2 + q_3) + I_{20} \sin(q_2 + q_3)],$$

$$c_{11} = -I_{20} \sin(q_2 + q_3) + I_{23} \sin(q_2 + q_3) + I_{19} \sin(q_2 + q_3),$$

$$c_{12} = -I_{11} \cos(q_3) - I_{12},$$

and the gravity vector $G(q)$ is written as

$$G(q) = \begin{bmatrix} 0 \\ G_2 \\ G_3 \\ 0 \\ G_5 \end{bmatrix}$$

where

$$\begin{aligned} G_2 &= g_1 \cos(q_2) + g_2 \sin(q_2 + q_3) + g_3 \sin(q_2) \\ &\quad + g_4 \cos(q_2 + q_3) + g_5 \sin(q_2 + q_3), \end{aligned}$$

$$G_3 = g_2 \sin(q_2 + q_3) + g_4 \cos(q_2 + q_3) + g_5 \sin(q_2 + q_3),$$

$$G_5 = g_5 \sin(q_2 + q_3).$$

Suppose the reference input trajectory is denoted by $q_d \in \mathbb{R}^5$, then the control objective of robot trajectory tracking is to make a robot position vector q following $q_d \in \mathbb{R}^5$.

Information about inertial constant and gravitational constant is shown in Tables 1 and 2.

Table 1

Inertial constant reference (kg m²).

$I_1 = 1.14 \pm 0.27$	$I_2 = 1.43 \pm 0.05$
$I_3 = 1.38 \pm 0.05$	$I_4 = 0.298 \pm 0.029$
$I_5 = -0.0213 \pm 0.0022$	$I_6 = -0.0142 \pm 0.0070$
$I_7 = -0.0001 \pm 0.0006$	$I_8 = 0.372 \pm 0.031$
$I_9 = -0.011 \pm 0.0011$	$I_{10} = 0.00125 \pm 0.0003$
$I_{11} = -0.0124 \pm 0.0003$	$I_{12} = 0.00058 \pm 0.00001$
$I_{13} = -0.69 \pm 0.02$	$I_{14} = 0.134 \pm 0.014$
$I_{15} = 0.238 \pm 0.012$	$I_{16} = 0.00379 \pm 0.0009$
$I_{17} = 0.000642 \pm 0.0003$	$I_{18} = 4.71 \pm 0.54$
$I_{19} = 1.75 \pm 0.07$	$I_{20} = 0.333 \pm 0.016$
$I_{21} = 0.000642 \pm 0.0003$	$I_{22} = 0.2 \pm 0.016$
$I_{23} = 0.00164 \pm 0.00007$	$I_{24} = 0.179 \pm 0.014$

Table 2

Gravitational constant (N m).

$g_1 = -37.2 \pm 0.5$	$g_2 = -8.43 \pm 0.20$
$g_3 = 1.02 \pm 0.50$	$g_4 = 0.249 \pm 0.025$
$g_5 = -0.0292 \pm 0.0056$	

3. Adaptive control of 5 DOF upper-limb exoskeleton robots with improved safety guarantees

3.1. Output tracking under uncertainties, parameter variance, and hardware malfunctions

To fulfill the tracking control objective, we first define the tracking error as $x_1 = q_d - q$, and its derivative as $x_2 = \dot{q}_d - \dot{q}$, then the state in the new coordinates is written as $x = [x_1^T x_2^T]^T$. Eq. (1) can be transformed into the following form:

$$M(x_1) \dot{x}_2 + C(x)x_2 + G(x_1) + \tau_d^* = \tau.$$

Then we have

$$\dot{x}_2 = -M^{-1}(x_1)[C(x)x_2 + G(x_1) + \tau_d^* - \tau],$$

where $u = -M^{-1}[C(x)x_2 + G(x_1) + \tau_d^* - \tau]$ is the control input. Assuming that the information of x and τ_d^* is exactly known, most of the existing results have extensively researched on the robotic control problem. Unfortunately, the parameter perturbations, actuator faults and hardware malfunctions in the practical application are inevitable. The uncertainties always cause the conventional robotic system design methods to lose effectiveness. Moreover, the full state measurement needs a sensor equipment that demands high investment and economic cost. Based on these considerations, we consider the uncertainties, parameter variance and actuator malfunctions in the following form:

$$\begin{aligned} \dot{x}_2 &= -M^{-1}(x_1)[C(x)x_2 + G(x_1) + F(x) + \tau_d^* - \tau] + \delta(t, x) \\ &= \rho(t)u + \delta(t, x), \quad \rho(t) > 0, \end{aligned}$$

where the term $\delta(t, x)$ represents the uncertainties and parameter variances and the unknown variable $\rho(t)$ is introduced to describe the changes in effectiveness caused by actuator faults and other malfunctions. Then adaptive control problem with improved safety requirement is especially taken into account for 5 DOF upper-limb exoskeleton robot. According to the result in [1], the uncertainties term $\delta(t, x)$ is written as

$$\delta(t, x) = D(x_1)x_1 + B(x_2)x_2 + Q,$$

where $K(x_1)$, $B(x_2)$, Q are norm-bounded terms. Thus, this paper considers that the uncertainties satisfy the following Assumptions 1 and 2.

Assumption 1. There are two *unknown* constants c and v such that

$$\|\delta(t, x)\| \leq c(\|x_1\| + \|x_2\|) + v.$$

Assumption 2. There is an *unknown* positive constant $\bar{\rho}$ such that $\rho(t) \geq \bar{\rho}$.

Remark 1. Assumptions 1 and 2 consider the uncertainties of linear growth form with an unknown rate and the bounded perturbations with a known bound. The prior knowledge is only the nominal model of the robotic system and the bound of the perturbations caused by actuator faults and other malfunctions.

In the following Section 3.2, we will first design a constant-gain controller for the case that $c, v, \bar{\rho}$ are known during the clinical operation for clarity. Then in Section 3.3, an adaptive mechanism will be proposed to handle the *unknown* uncertainty-case under Assumptions 1 and 2.

3.2. Trajectory tracking controller design with constant gain in known parameters case

Let us introduce the following notations:

$$A = \begin{bmatrix} 0_{5 \times 5} & I_{5 \times 5} \\ 0_{5 \times 5} & 0_{5 \times 5} \end{bmatrix}, \quad B = \begin{bmatrix} 0_{5 \times 5} \\ I_{5 \times 5} \end{bmatrix}, \quad C = [0_{5 \times 5} \quad I_{5 \times 5}].$$

Then the 5 DOF robotic system (1) with uncertainties is transformed into the following form:

$$\begin{aligned} \dot{x} &= Ax + B\rho(t)u + B\delta(t, x) \\ y &= Cx. \end{aligned} \quad (2)$$

For systems (2), we first propose a high-gain dynamic output feedback controller and show that it can globally exponentially stabilize system (2) by properly choosing high-gain parameters. The proposed output feedback controller has the following form.

Tracking error feedback controller:

$$\begin{aligned} u &= K(\varepsilon)\hat{x} \\ \dot{\hat{x}} &= A\hat{x} + Bu - L(\varepsilon)(y - C\hat{x}), \end{aligned} \quad (3)$$

where $K(\varepsilon) \triangleq [(k_1/\varepsilon^2)I_{5 \times 5}, (k_2/\varepsilon)I_{5 \times 5}]$, $L(\varepsilon) \triangleq [(l_1/\varepsilon)I_{5 \times 5}, (l_2/\varepsilon^2)I_{5 \times 5}]^T$ and $\varepsilon > 0$. k_1, k_2, l_1, l_2 and ε are the parameters to be designed.

The following lemma shows that for *known* parameters c, v and ρ , the above controller can stabilize the 5 DOF robotic system (1) with properly selected constant parameters k_1, k_2, l_1, l_2 and ε .

Denote

$$\begin{aligned} K &= K(1), \quad L = L(1), \quad A_K(\varepsilon) = A + BK(\varepsilon), \\ A_L(\varepsilon) &= A + L(\varepsilon)C, \quad E(\varepsilon) = \text{diag}[I_{5 \times 5}, \varepsilon I_{5 \times 5}], \\ A_K &= A_K(1) = A + BK(1) = A + BK, \\ A_L &= A_L(1) = A + L(1)C = A + LC. \end{aligned}$$

Lemma 1. Suppose that c, v and ρ are known. Select the values for k_1, k_2, l_1 and l_2 such that both matrices A_K and A_L are Hurwitz, respectively. Then, there exists a constant $\varepsilon^* > 0$ such that for $0 < \varepsilon < \varepsilon^*$, systems (2) and (3) are ultimately stable, and $\|x_1 - \hat{x}_1\|$ has a tunable bound.

Proof. Define the state estimate error as $e = x - \hat{x}$. Then the error dynamics is

$$\dot{e} = A_L(\varepsilon)e + (1 - \rho(t))BK(\varepsilon)\hat{x} + \delta(t, x).$$

Note that $A_L = \begin{bmatrix} l_1 & 1 \\ l_2 & 0 \end{bmatrix} \otimes I_5$. The eigenvalues of A_L are determined by l_1 and l_2 . By properly selecting l_1 and l_2 , A_L is Hurwitz and satisfying the Lyapunov equation with a symmetric positive definite matrix P_L

$$A_L^T P_L + P_L A_L = -I.$$

Note that $A_L(\varepsilon) = E(\varepsilon)^{-1} A_L E(\varepsilon)$, one obtains a new Lyapunov equation

$$A_L(\varepsilon)^T P_L(\varepsilon) + P_L(\varepsilon) A_L(\varepsilon) = -\varepsilon^{-1} E(\varepsilon)^2,$$

where $P_L(\varepsilon) = E(\varepsilon) P_L E(\varepsilon)$. Define a Lyapunov function $V_o(e) = e^T P_L(\varepsilon) e$, along the trajectory of error dynamics, considering $\|E(\varepsilon)\delta(t, x)\| \leq \sqrt{n}c\|E(\varepsilon)x\| + \varepsilon cv$, the time derivative of $V_o(e)$ is written as

$$\begin{aligned} \dot{V}_o(e) &\leq -(\varepsilon^{-1} - 2|1 - \rho(t)|\|P_L\|\|BK\|)\|E(\varepsilon)e\|^2 + 2\sqrt{nc}\|P_L\|\|E(\varepsilon)e\|\|E(\varepsilon)x\| \\ &\quad + 2\varepsilon cv\|P_L\|\|E(\varepsilon)e\| + 2\varepsilon^{-1}|1 - \rho(t)|\|P_L\|\|BK\|\|E(\varepsilon)e\|\|E(\varepsilon)x\|. \end{aligned}$$

The closed-loop system is written in the following compact form:

$$\dot{x} = A_K(\varepsilon)x - (1 - \rho(t))BK(\varepsilon)x - \rho(t)BK(\varepsilon)e + \delta(t, x).$$

Note that $A_K = \begin{bmatrix} 0 & 1 \\ k_1 & k_2 \end{bmatrix} \otimes I_5$. The eigenvalues of A_K are determined by k_1 and k_2 . By selecting k_1 and k_2 satisfying A_K is Hurwitz, one can build a Lyapunov equation with a symmetric positive definite matrix P_K

$$A_K^T P_K + P_K A_K = -I.$$

Note that $A_K(\varepsilon) = E(\varepsilon)^{-1} A_K E(\varepsilon)$, one obtains a new Lyapunov equation

$$A_K(\varepsilon)^T P_K(\varepsilon) + P_K(\varepsilon) A_K(\varepsilon) = -\varepsilon^{-1} E(\varepsilon)^2,$$

where $P_K(\varepsilon) = E(\varepsilon) P_K E(\varepsilon)$. Thus, one obtains a new Lyapunov function $V_c(x) = x^T P_K(\varepsilon) x$. Now, along the trajectory, noting that $E(\varepsilon)BK(\varepsilon)e = \varepsilon^{-1} BKE(\varepsilon)e$, the time derivative of $V_c(x)$ is computed as the following equation:

$$\begin{aligned} \dot{V}_c(x) &\leq -\{\varepsilon^{-1} - 2\sqrt{n}\|P_K\|c - 2|1 - \rho(t)|\|P_K\|\|BK\|\}\|E(\varepsilon)x\|^2 \\ &\quad + 2\varepsilon^{-1}\rho(t)\|P_K\|\|BK\|\|E(\varepsilon)x\|\|E(\varepsilon)e\| + 2\varepsilon\sqrt{ncv}\|P_K\|\|E(\varepsilon)x\|. \end{aligned}$$

Now, let us define a composite Lyapunov function $V(e, x) = dV_o(e) + \varepsilon V_c(x)$, $d > 0$, for the closed-loop system. Then, one has

$$\dot{V}(e, x) \leq -\sum(\varepsilon)^T T(\varepsilon) \sum(\varepsilon) + 2\varepsilon cv\|P_L\|\|E(\varepsilon)e\| + 2\sqrt{ncv}\|P_K\|\|E(\varepsilon)x\|,$$

where

$$T(\varepsilon) = \begin{bmatrix} d(\varepsilon^{-1} - 2|1 - \rho(t)|\|P_L\|\|BK\|) & \Lambda \\ \Lambda & \varepsilon\{\varepsilon^{-1} - 2\sqrt{n}\|P_K\|c - 2|1 - \rho(t)|\|P_K\|\|BK\|\} \end{bmatrix},$$

$$\Lambda = -\|P_K\|\|K\| - d\sqrt{nc}\|P_L\| + 2|1 - \rho(t)|\|P_L\|\|BK\| + 2\rho(t)\|P_K\|\|BK\|,$$

$$\sum(\varepsilon) = \begin{bmatrix} \|E(\varepsilon)e\| \\ \|E(\varepsilon)x\| \end{bmatrix}.$$

Then one has

$$\begin{aligned} \sqrt{\|E(\varepsilon)e\|^2 + \|E(\varepsilon)x\|^2} &\leq \sqrt{\frac{M}{m}} \sqrt{\|E(\varepsilon)e\|^2 + \|\sqrt{\varepsilon}E(\varepsilon)x\|^2} e^{-(\lambda_{\min}(R_k)/2M)t} \\ &\quad + \frac{M\sqrt{2}}{\pi_k} \left(1 - e^{-(\pi_k/2M)(t-t_k)}\right), \end{aligned}$$

if and only if the equation $0 < \varepsilon < \varepsilon^*$ where ε^* satisfies that $T(\varepsilon^*)$ is positive definite. Thus one has

$$\begin{aligned} \|x_1 - \hat{x}_1\| &\leq \|E(\varepsilon_j)e\| + \|\sqrt{\varepsilon_j}E(\varepsilon_j)x\| \\ &\leq \sqrt{n} \sqrt{\frac{M}{m}} \sqrt{\|E(\varepsilon_k)e\|^2 + \|\sqrt{\varepsilon_k}E(\varepsilon_k)x\|^2} e^{-(\lambda_{\min}(R_k)/2M)t} + M\sqrt{2n}\varepsilon_j\varsigma, \end{aligned}$$

where $\varsigma = \max\{\varepsilon\|P_L\|, \|P_K\|\}$. This completes the proof of Lemma 1. \square

Remark 2. According to Lemma 1, in the presence of uncertainties and nonlinearities satisfying Assumptions 1 and 2 but with unknown constants c, v and ρ , the controller (3) with an approximate value of gain-like parameter ε is robust to all such uncertainties and faults.

Remark 3. Because the uncertainties in Assumption 1 is in an unknown linear growth form, inappropriate (not small enough) values of the gain-like parameter cannot guarantee the stability of

the closed-loop system. From the derivation of Lemma 1, inappropriate values of ε result in matrix non-positive definite $T(\varepsilon)$ or even negative definite. Then the stability of closed-loop system cannot be achieved.

3.3. Trajectory tracking controller design with tuning mechanism for unknown uncertainties and faults

To implement controller (3), we need to choose ε requiring a priori knowledge of c , v and ρ . Moreover, when the system nonlinearities change, we need to tune the high-gain parameter ε accordingly if necessary. In the following, we introduce an adaptive controller which can tune the high gain parameter online depending on the information of system nonlinearities and faults or hardware malfunctions.

Adaptive output feedback controller:

$$\begin{aligned} u &= K(\varepsilon(t))\hat{x} \\ \dot{\hat{x}} &= A\hat{x} + Bu - L(\varepsilon(t))(y - C\hat{x}), \end{aligned} \quad (4)$$

where the time-varying gain matrices $K(\varepsilon(t))$ and $L(\varepsilon(t))$ are introduced as

$$K(\varepsilon(t)) = [k_1/\varepsilon(t)^2 I_{5 \times 5}, k_n/\varepsilon(t) I_{5 \times 5}], \quad L(\varepsilon(t)) = [l_1/\varepsilon(t) I_{5 \times 5}, l_n/\varepsilon(t)^2 I_{5 \times 5}]^T.$$

The parameter $\varepsilon(t)$ is tuned according to the following switching mechanism.

Switching mechanism with improved safety:

$$\dot{\theta}(t) = \mu \|x_1(t) - \hat{x}_1(t)\| - 2\mu M\zeta\varepsilon, \quad \theta(t_0) = \theta_0.$$

Update law: Initialization: set $T_0 = \theta_0 > 0$ and $i = 0$.

Step 1: $T_{i+1} = aT_i$, $a > 1$. Set $\varepsilon(t) = 1/(\sigma T_i)$.

Step 2: If $\theta(t) > T_{i+1}$,

Then $\varepsilon(t) = 1/(\sigma T_{i+1})$, $i = i + 1$, go to Step 1;

Else $\varepsilon(t) = 1/(\sigma T_i)$, go to Step 2;

where the parameter $\sigma = 2\sqrt{n}\|P_K\| + 4\sqrt{n}\|K\|\|P_K\|\|P_L\|$.

Remark 4. The intuitional idea of switching mechanism with the update law is two-fold: First, $\varepsilon(t)$ is a monotonically nondecreasing function of time by taking integral value of $\mu \|x_1(t) - \hat{x}_1(t)\| - 2\mu M\zeta\varepsilon$. Obviously, $\theta(t)$ stops increasing only when $\|x_1(t) - \hat{x}_1(t)\| \leq 2M\zeta\varepsilon$. Also, from the switching logic, it can be seen that $T(t)$ is a piecewise constant function of time and increases stepwise with some time-interval. At some point of switching time, $T(t)$ will be tuned sufficiently large such that during each time interval, Lemma 1 can be applied for each switched subsystem. With this, the increment of $\theta(t)$ may become smaller and eventually there would be the last switching point. After the last switching occurs, the proposed controller (4) becomes the same one as the static case of controller (3). Overall, the proposed scheme leads to a switched nonlinear system.

Theorem 1. Suppose that Assumptions 1 and 2 hold, select k_1, k_2, l_1, l_2 such that both matrix $A_K = A + BK$ and $A_L = A + LC$ are Hurwitz. Then, the closed-loop system (2) with controller (4) is globally asymptotically stable, and the tracking error $\|x_1(t) - \hat{x}_1(t)\|$ has a tunable bound.

Proof. First, note that the uncertainty $\delta(t, x)$ satisfies the global linear growth condition. Thus, there is no finite escape phenomenon with the proposed controller (4). Consider a case that $q(t)$ increases along the time. Then, there exists a switching time t_j , i.e., a time at which such that T_j is large enough that the conclusion of Lemma 1 holds for each interval $\Delta t_k = [t_k, t_{k+1}]$. Now, one only needs to consider the case of $t \geq t_j$. Note that for each time-interval Δt_k , $k \geq j$, $T(t)$ remains as a constant value T_k .

Thus, as a whole, the closed-loop system can be viewed as a switched system $\dot{x} = f_k(x, u)$, $k = j, j+1, \dots, l$ and for each time-interval Δt_k , each subsystem $\dot{x} = f_k(x, u)$ is engaged. In the following, we will prove that l is indeed a finite number. For each subsystem $\dot{x} = f_k(x, u)$, utilizing the proof of Lemma 1, one can set a Lyapunov function

$$V_k(e, x) = dV_o(e) + \varepsilon_k V_{ck}(x)$$

where $V_{ok}(e) = e^T P_L(\varepsilon_k) e$, $V_{ck}(x) = x^T P_K(\varepsilon_k) x$ and ε_k is a sufficiently small constant. Recall that $P_L(\varepsilon_k) = E(\varepsilon_k) P_L E(\varepsilon_k)$, $P_K(\varepsilon_k) = E(\varepsilon_k) P_K E(\varepsilon_k)$, where $E(\varepsilon) = \text{diag}[I_{5 \times 5}, \varepsilon I_{5 \times 5}]$. Then, one can show

$$m(\|E(\varepsilon_k)e\|^2 + \|\sqrt{\varepsilon_k}E(\varepsilon_k)x\|^2) \leq V_k(e, x) \leq M(\|E(\varepsilon_k)e\|^2 + \|\sqrt{\varepsilon_k}E(\varepsilon_k)x\|^2)$$

where $m = \min\{\lambda_{\min}(P_L), \lambda_{\min}(P_K)\}$, $M = \max\{\lambda_{\max}(P_L), \lambda_{\max}(P_K)\}$. For a sufficiently small constant, we already have

$$\begin{aligned} \dot{V}_k(e, x) &\leq -\sum(\varepsilon_k)^T T(\varepsilon_k) \sum(\varepsilon_k) + 2\varepsilon_k c v \|P_L\| \|E(\varepsilon_k)e\| \\ &\quad + 2\sqrt{n} c v \|P_K\| \|E(\varepsilon_k)x\|, \end{aligned}$$

where

$$T(\varepsilon) = \begin{bmatrix} d(\varepsilon^{-1} - 2|1 - \rho(t)|\|P_L\|\|BK\|) & \Lambda \\ \Lambda & \varepsilon\{\varepsilon^{-1} - 2\sqrt{n}\|P_K\|c - 2|1 - \rho(t)|\|P_K\|\|BK\|\} \end{bmatrix},$$

$$\Lambda = -\|P_K\|\|K\| - d\sqrt{n}c\|P_L\| + 2|1 - \rho(t)|\|P_L\|\|BK\| + 2\rho(t)\|P_K\|\|BK\|,$$

$$\sum(\varepsilon) = \begin{bmatrix} \|E(\varepsilon)e\| \\ \|E(\varepsilon)x\| \end{bmatrix}.$$

Then

$$\begin{aligned} &\sqrt{\|E(\varepsilon_k)e\|^2 + \|E(\varepsilon_k)x\|^2} \\ &\leq \sqrt{\frac{M}{m}} \sqrt{\|E(\varepsilon_k)e\|^2 + \|\sqrt{\varepsilon_k}E(\varepsilon_k)x\|^2} e^{-(\lambda_{\min}(R_k)/2M)t} \\ &\quad + \frac{M\sqrt{2}}{\pi_k} \left(1 - e^{-(\pi_k/2M)(t-t_k)}\right) \end{aligned}$$

is rewritten as

$$\begin{aligned} &\sqrt{\|E(\varepsilon_k)e\|^2 + \|E(\varepsilon_k)x\|^2} \leq \rho_k e^{-\pi_k t} + \frac{M\sqrt{2}}{\pi_k} \left(1 - e^{-(\pi_k/2M)(t-t_k)}\right), \\ &\rho_k > 0, \quad \pi_k > 0, \end{aligned}$$

and

$$\begin{aligned} &\|E(\varepsilon_j)e\|^2 + \|\sqrt{\varepsilon_j}E(\varepsilon_j)x\|^2 \\ &\leq \sqrt{2} \sqrt{\frac{M}{m}} \sqrt{\|E(\varepsilon_k)e\|^2 + \|\sqrt{\varepsilon_k}E(\varepsilon_k)x\|^2} e^{-(\lambda_{\min}(R_k)/2M)t} + M\sqrt{2n}\varepsilon\zeta, \end{aligned}$$

where $\zeta = \max\{\varepsilon\|P_L\|, \|P_K\|\}$. Here, ρ_k is a nonincreasing sequence with respect to index k . When ε_k is sufficiently small, for each fixed ε_k ,

$$\begin{aligned} \|x_1 - \hat{x}_1\| &\leq \|E(\varepsilon_k)e\| + \|\sqrt{\varepsilon_k}E(\varepsilon_k)x\| \\ &\leq \sqrt{2} \sqrt{\|E(\varepsilon_k)e\|^2 + \|\sqrt{\varepsilon_k}E(\varepsilon_k)x\|^2} + 2M\varepsilon\zeta \\ &\leq \sqrt{2}\rho_k e^{-\pi_k t} + 2M\varepsilon\zeta. \end{aligned}$$

From $\dot{q}(t) = \mu \|x_1(t) - \hat{x}_1(t)\| - 2\mu M\zeta\varepsilon$, one has $\dot{q}(t) \leq \mu\sqrt{2}\rho_k e^{-\pi_k t}$ for $t \in \Delta t_k$, with $q(t_k) = q_k$. Since $q(t)$ is a monotonically nondecreasing function, the increment of $q(t)$ for $t \in \Delta t_k$ is computed as $\Delta q(\Delta t_k) = \int_{t_k}^{t_{k+1}} \dot{q}(\tau) d\tau \leq (\mu\sqrt{2}\rho_k/\pi_k)(e^{-\pi_k t_k} - e^{-\pi_k t_{k+1}})$.

Furthermore, the increment of sequence R_k is $\Delta R_k = R_{k+1} - R_k = a^k(a-1)R_0$, $a > 1$. According to the switching logic, it is obvious that there exists a finite time t_l , $l \geq j$, such that t_l would be the last switching time. Therefore, the switched system consists of only a finite number of subsystems. According to the result in [13], one can obtain the minimum holding time $H_k \geq (1/\pi_k) \ln(\sqrt{M/m})$. Then one can obtain the redundancy $r_k = \Delta t_k - H_k$ for each time interval.

With π_k remaining bounded due to the fact that l is finite, one has $\sum_{k=j}^l \pi_k r_k = \infty$. Thus, the closed-loop switched system is globally asymptotically stable. Finally, utilizing Barbalat's lemma, one concludes that $q(t)$ converges to $q_{ss} < \infty$ as $t \rightarrow \infty$ by the proposed scheme. One can conclude that $\|x_1(t) - \hat{x}_1(t)\|$ has a tunable bound $\sqrt{2M_{\xi}\varepsilon}$. \square

Remark 5. By utilizing the adaptive controller (4) with dynamic gain $\varepsilon(t)$. The appropriate choice of parameters in the tuning mechanism can guarantee that after a finite number of switching all closed-loop signals will have exponential convergence in the presence of the nonlinearity and faults in the closed-loop system. From the derivation of Theorem 1, we can see that selection of more smaller ε will shorten the time of the transient process before the exponential convergence. But ε should not be too small and reduced too fast to avoid the possible disturbance sensitivity. In application, the value of parameter $a > 1$ in the switch mechanism should not be too large to avoid the performance degradation. To give more safety constraints, the techniques of Barrier Lyapunov functions in [22–24] might be useful and more involved as a further research objective.

4. Experimental results and discussion

In this section, we will evaluate the proposed adaptive control approach with improved safety requirement on the 5 DOF upper-limb exoskeleton robot model [15,16]. To testify the proposed

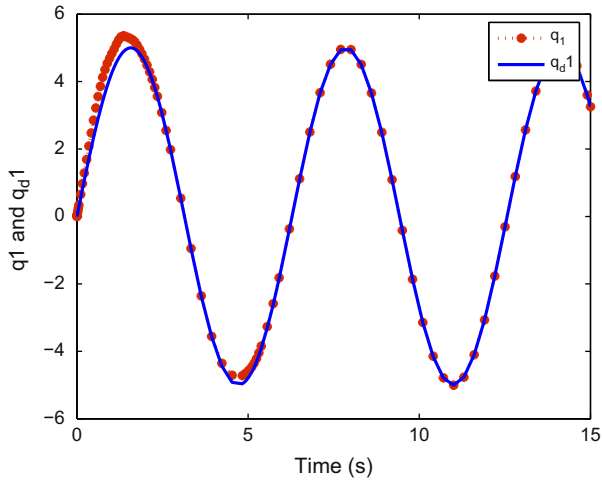


Fig. 3. The position tracking of q_1 to the desired trajectory q_{d1} (m).

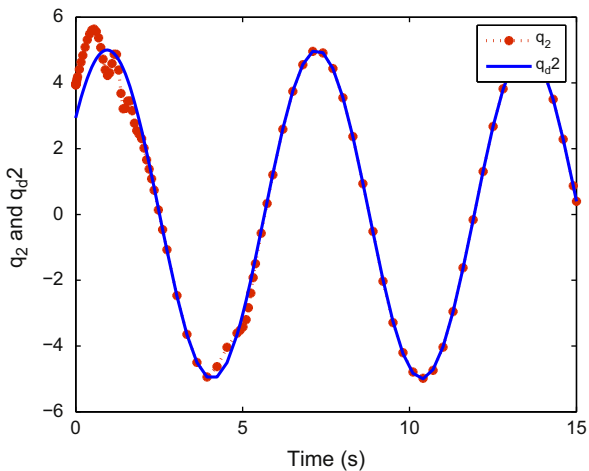


Fig. 4. The position tracking of q_2 to the desired trajectory q_{d2} (m).

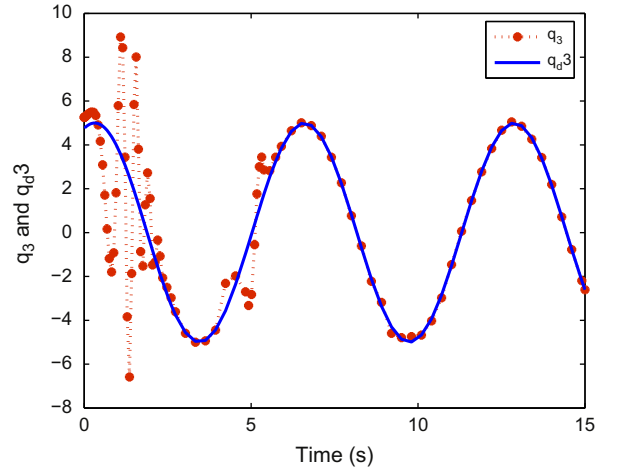


Fig. 5. The position tracking of q_3 to the desired trajectory q_{d3} (m).

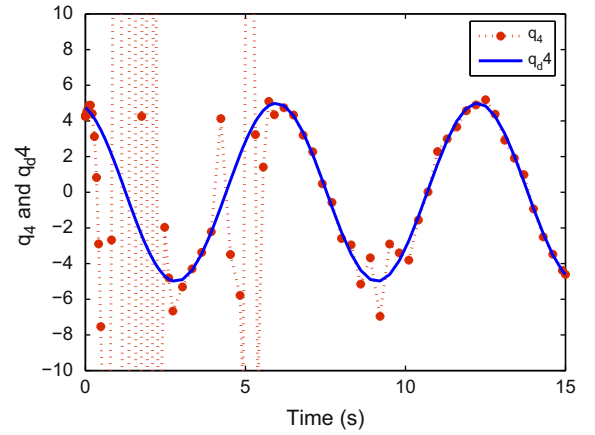


Fig. 6. The position tracking of q_4 to the desired trajectory q_{d4} (m).

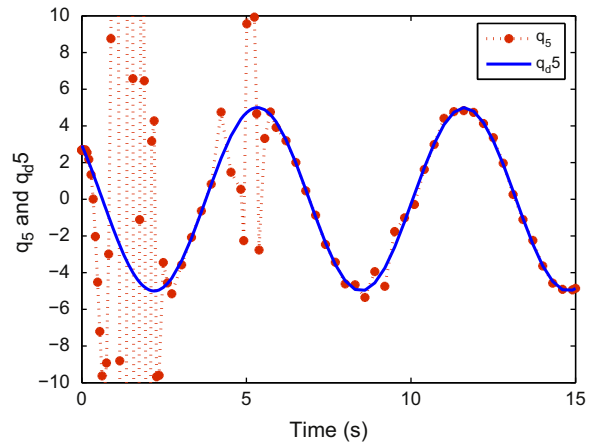


Fig. 7. The position tracking of q_5 to the desired trajectory q_{d5} (m).

adaptive safety-improved controller, the desired trajectory $q_d = [q_{d1}, q_{d2}, q_{d3}, q_{d4}, q_{d5}]^T$ of $q = [q_1, q_2, q_3, q_4, q_5]^T$ is chosen as the following equations $q_{di} = \sin(t + i\pi/5)$, $i = 1, \dots, 5$. The trajectory tracking error bound of $q_d = [q_{d1}, q_{d2}, q_{d3}, q_{d4}, q_{d5}]^T$ is chosen as 0.1 mm. The initial state of the robotic system is $q_d = [0, 4, 5.5, 5.5, 5]^T$. The initial gain parameter is $\varepsilon(0) = 0.5$.

Figs. 3–7 show the tracking response curves of position trajectories $q_d = [q_{d1}, q_{d2}, q_{d3}, q_{d4}, q_{d5}]^T$. It can be seen that our

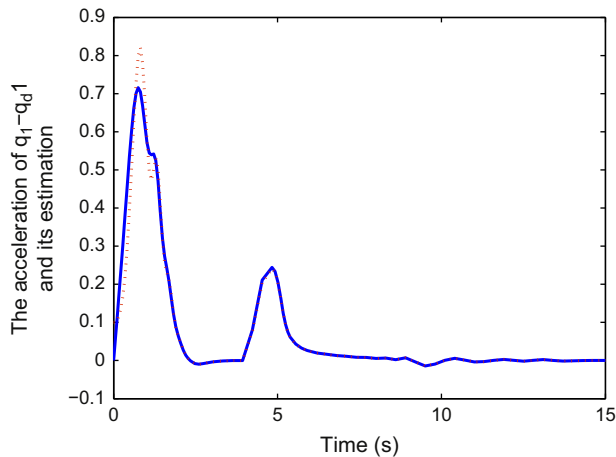


Fig. 8. The acceleration of $\dot{q}_1 - \dot{q}_{d1}$ (solid) and its estimation (dot) provided by adaptive observer (m/s).

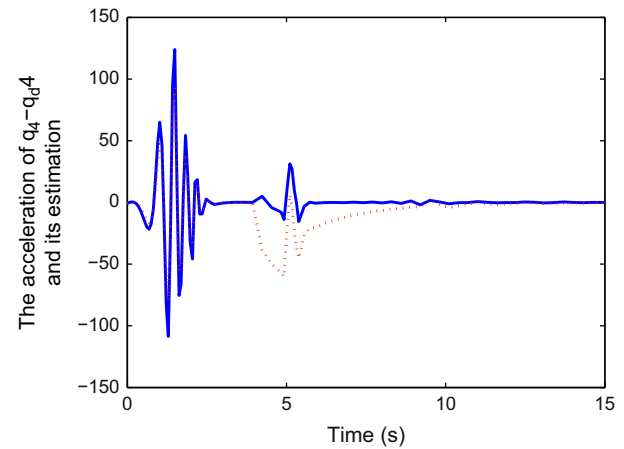


Fig. 11. The acceleration of $\dot{q}_4 - \dot{q}_{d4}$ (solid) and its estimation (dot) provided by adaptive observer (m/s).

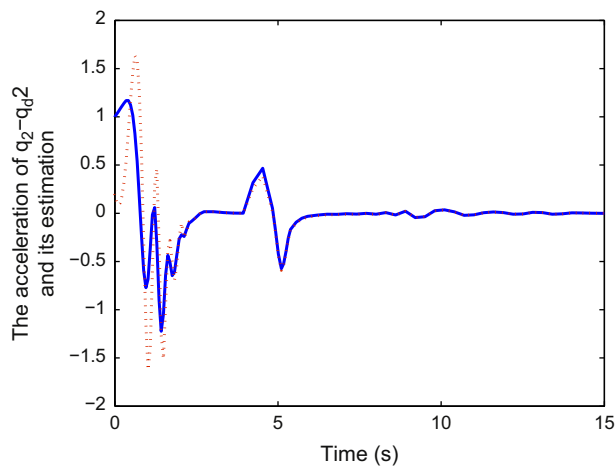


Fig. 9. The acceleration of $\dot{q}_2 - \dot{q}_{d2}$ (solid) and its estimation (dot) provided by adaptive observer (m/s).

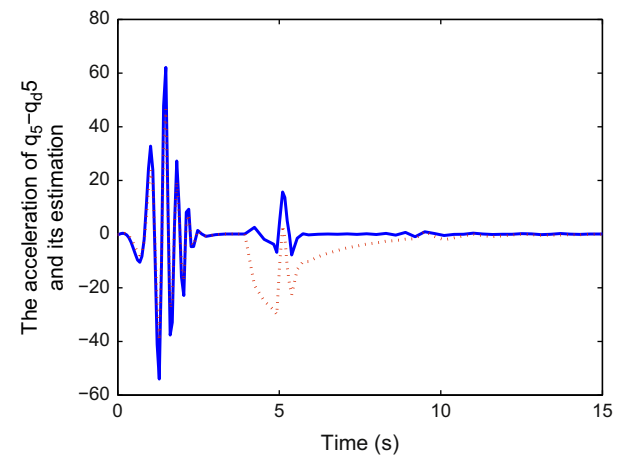


Fig. 12. The acceleration of $\dot{q}_5 - \dot{q}_{d5}$ (solid) and its estimation (dot) provided by adaptive observer (m/s).

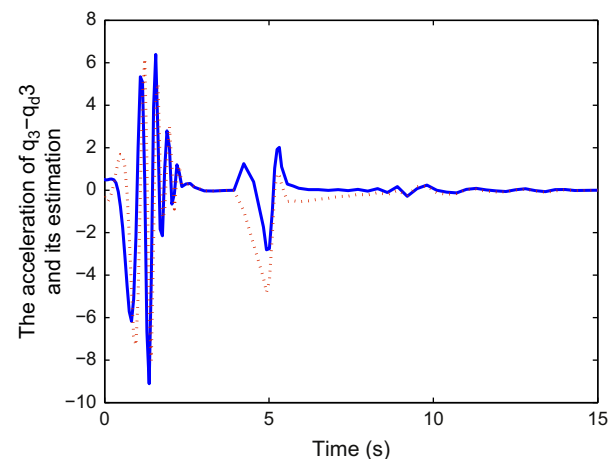


Fig. 10. The acceleration of $\dot{q}_3 - \dot{q}_{d3}$ (solid) and its estimation (dot) provided by adaptive observer (m/s).

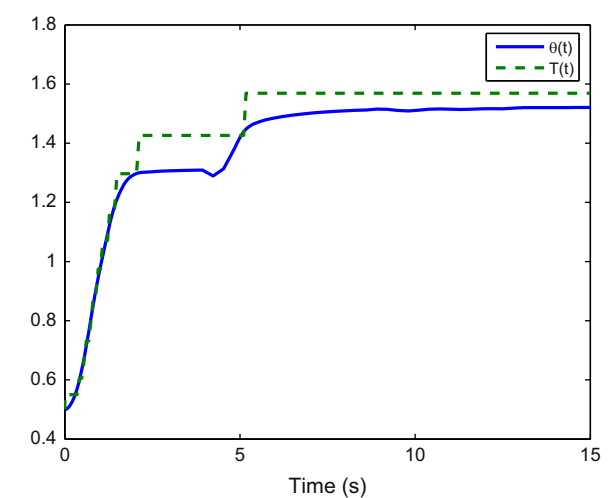


Fig. 13. The signals in the switching mechanism of the adaptive robust controller $T(t)$ and q .

controller will guarantee that the unknown uncertainties can be accumulated despite that the available information is only the position tracking error. By the information of the accelerations of $\dot{q}_i - \dot{q}_{di}$, $i = 1, \dots, 5$ from the adaptive observer, the output feedback controller excellently works. In Figs. 8–12, the accelerations of

$\dot{q}_i - \dot{q}_{di}$, $i = 1, \dots, 5$ are estimated in less than 10 s. Both the position tracking error and the corresponding acceleration estimation errors exponentially converge to zero after several adjustments in the gain of controller and observer. In less than 3.5 s, the effect

of uncertainties has been accommodated. All the signals remain bounded in a reasonable interval during operation. Especially, the tracking error bound is guaranteed when the robotic systems run into the stationary situation. The signals used in the switching mechanism are shown in Fig. 13, which can clearly show the comparisons between $T(t)$ and $\theta(t)$ and the switching increasing of $T(t)$. When the value of $\theta(t)$ is large than $T(t)$, then the value of $\theta(t)$ increases. When $\theta(t)$ is larger than $T(t)$, the switches occur with enlarging $T(t)$ exponentially, which results in reducing the value of the gain-like parameter ε . Although the value of $T(t)$ frequently jumps, the continuity of all signals in controller and observer is guaranteed (see Fig. 14). To show the ability of the adjustment of the adaptive controller, at $t = 4$, the parameter of τ^* is perturbed by friction torque 0.5 N m and $\rho(t) = 1.2$. Then the gain-related parameter $\varepsilon(t)$ is readjusted such that the stability is recovered. The input is shown in Fig. 15. The process of the fault accommodation

can be clearly shown by the changes of the signals in the turning mechanism. As a comparison, Fig. 16 shows the response curve of $q_1 - q_d$ without the adaptive mechanism of the proposed control scheme.

5. Concluding remarks

A novel safety-improved adaptive controller design method for 5 DOF upper-limb exoskeleton robot was developed in this work. Compared with the existing results, our control strategy does not impose the measurement of velocity and acceleration, what is more, the uncertainties and hardware malfunctions are taken into consideration for more practical application. By constructing a gain updating mechanism, the effect of uncertainties, unknown

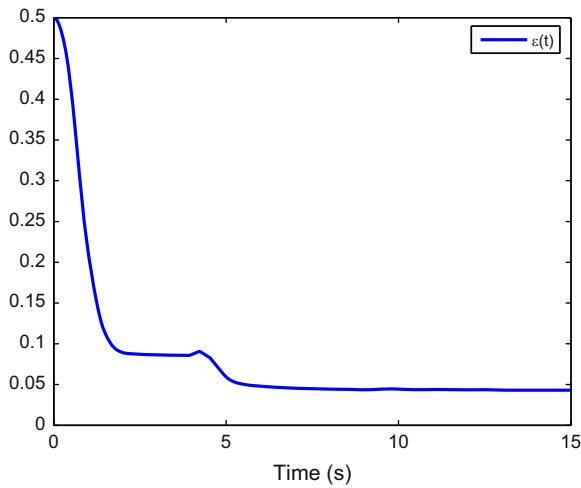


Fig. 14. The gain $\varepsilon(t)$ in the adaptive robust controller.

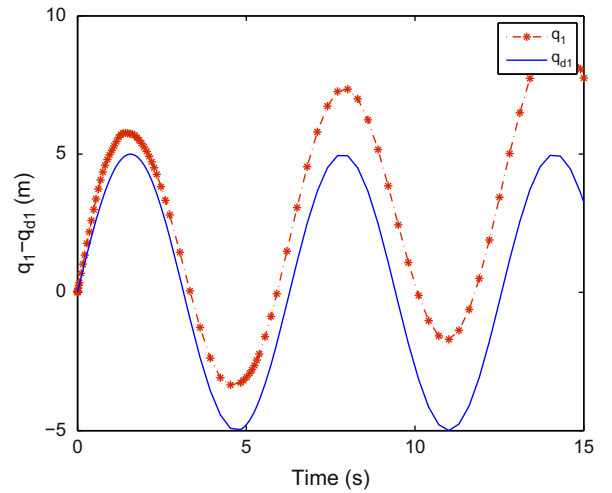


Fig. 16. The position tracking of q_1 to the desired trajectory q_{d1} (m) without adaptive mechanism.

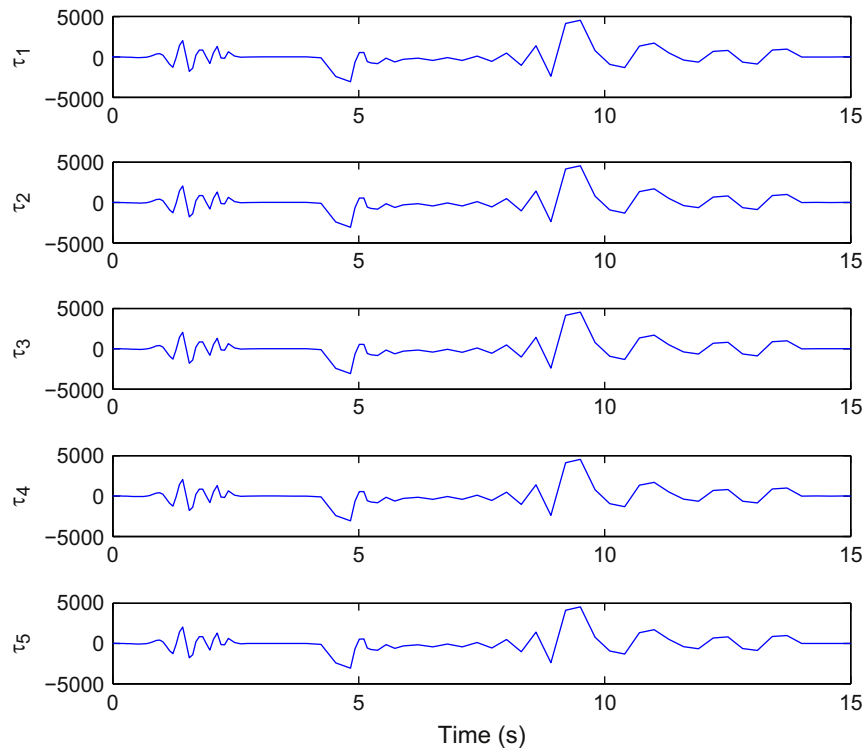


Fig. 15. The input in the adaptive robust controller (N m).

parameter perturbations and hardware malfunctions can be automatically accommodated along with a finite number of adjustments. In 5 DOF upper-limb exoskeleton robotic system, the experimental results demonstrate the feasibility of the proposed adaptive robust control strategy. The user can easily achieve trajectory planning using intuitive, simple and low-cost technology. Precise motion position technology with safety protection is the goal we are currently pursuing.

References

- [1] Prange GB, Jannick MA, Groothuis-Oudshoorn CGM, Hermens H, Ijzerman MJ. Systematic review of the effect of robot-aided therapy on recovery of the hemiparetic arm after stroke. *Journal of Rehabilitation Research and Development* 2006;43(2):171–84.
- [2] Kwakkel G, Kollen BJ, Krebs HI. Effects of robot assisted therapy on upper limb recovery after stroke: a systematic review. *Neurorehabilitation & Neural Repair* 2008;22(2):111–21.
- [3] Hendricks HT, van Limbeek J, Geurts AC, Zwarts MJ. Motor recovery after stroke: a systematic review of the literature. *Archives of Physical Medicine and Rehabilitation* 2002;83(11):1629–37.
- [4] Hunt KJ, Muni H, de Donaldson N. Feedback control of unsupported standing in paraplegia. Part I. Optimal control approach. *IEEE Transactions on Rehabilitation Engineering* 1997;5(4):331–40.
- [5] Hunt KJ, Jaime RP, Gollee H. Robust control of electrically stimulated muscle using polynomial H_∞ design. *Control Engineering Practice* 2001;9(3):313–28.
- [6] Yu W, Rosen J. A novel linear PID controller for an upper limb exoskeleton. In: 2010 49th IEEE conference on decision and control, CDC 2010, December 15, 2010–December 17, 2010. Atlanta, GA, United states; 2010. p. 3548–53.
- [7] Nef T, Mihelj M, Riener R. ARMin: a robot for patient cooperative arm therapy. *Medical & Biological Engineering & Computing* 2007;45(September):887–900.
- [8] Jezernik S, Wassink RGV, Keller T. Sliding mode closed-loop control of FES: controlling the shank movement. *IEEE Transactions on Biomedical Engineering* 2004;51(2):263–72.
- [9] Freeman CT, Hughes A-M, Burrage JH, Chappell PH, Lewin PL, Rogers E. Iterative learning control of FES applied to upper extremity for rehabilitation. *Control Engineering Practice* 2009;17(3):368–81.
- [10] Previdi F, Carpanzano E. Design of a gain scheduling controller for knee-joint angle control by using functional electrical stimulation. *IEEE Transactions on Control Systems Technology* 2003;11(3):310–24.
- [11] Krstic M, Kanellakopoulos I, Kokotovic P. *Nonlinear and adaptive control*. New York: Wiley; 1995.
- [12] Spong MW, Vidyasagar M. *Robot dynamics and control*. New York: Wiley; 1989.
- [13] Ma HJ, Yang GH. Adaptive logic-based switching fault-tolerant controller design for nonlinear uncertain systems. *International Journal of Robust and Nonlinear Control* 2011;21(4):404–28.
- [14] Jin XZ, Yang GH. Robust adaptive fault-tolerant compensation control with actuator failures and bounded disturbances. *Acta Automatica Sinica* 2009;35(3):305–9.
- [15] Asada H, Youcef-Toumi K. Analysis and design of a direct-drive arm with a five-bar-link parallel drive mechanism. *ASME Journal of Dynamic Systems, Measurement, and Control* 1984;106(September):225–30.
- [16] Li QL, Wang DY, Du ZJ, Sun YSLN. sEMG based control for 5 DOF upper limb rehabilitation robot system, robotics and biomimetics, ROBIO '06. In: IEEE international conference on digital object identifier; 2006. p. 1305–10.
- [17] Tong S, Li Y. Observer-based fuzzy adaptive control for strict-feedback nonlinear systems. *Fuzzy Sets and Systems* 2009;160(12):1749–64.
- [18] Li Y, Tong S, Li T. Adaptive fuzzy output feedback control for a single-link flexible robot manipulator driven DC motor via backstepping. *Nonlinear Analysis: Real World Applications* 2013;14(1):483–94.
- [19] Tong S, Liu C, Li Y. Fuzzy-adaptive decentralized output-feedback control for large-scale nonlinear systems with dynamical uncertainties. *IEEE Transactions on Fuzzy Systems* 2010;18(5):845–61.
- [20] Tong S, He X, Zhang H. A combined backstepping and small-gain approach to robust adaptive fuzzy output feedback control. *IEEE Transactions on Fuzzy Systems* 2009;17(5):1059–69.
- [21] Li Y, Tong S, Li T. Adaptive fuzzy output feedback control of uncertain nonlinear systems with unknown backlash-like hysteresis. *Information Sciences* 2012;198:130–46.
- [22] Tee KP, Ge SS, Tay EH. Barrier Lyapunov functions for the output constrained nonlinear systems. *Automatica* 2009;45(4):918–27.
- [23] Benchliousis CP, Rovithakis GA. Robust adaptive control of feedback linearizable MIMO nonlinear systems. *IEEE Transactions on Automatic Control* 2008;53(9):2090–9.
- [24] Hackl CM. High-gain position control. *International Journal of Control* 2011;84(10):1695–716.